J Therm Anal Calorim (2010) 101:965–971
DOI 10.1007/s10973-009-0631-1

Differential thermal analysis of a zeolite Y crystalline structure in a catalyst

Maria Luisa A. Gonçalves · Meri D. Vieira ·
Deusa Angélica P. Mota · Wildson V. Cerqueira ·
Ana Maria R. F. Teixeira

Received: 12 October 2009 / Accepted: 2 December 2009 / Published online: 5 January 2010

Abstract The purpose of this work was to employ the differential thermal analysis (DTA) technique to compare variations in the collapse energy of the zeolite Y crystalline structure in a fresh catalyst and in the same catalyst impregnated with nickel and vanadium. A small exothermic signal in the DTA curve at 950–1150 °C indicated the collapse of the crystalline structure. The areas of the exothermic signals in the DTA curves of the two samples indicated a reduction in the curve of the metal impregnated catalyst. These results were compared with X-ray data, leading to the conclusion that metal impregnation affects the zeolite Y crystalline structure and that the DTA technique is a potentially useful tool for measuring the integrity of zeolite Y in catalysts.

Keywords Catalyst · Zeolite Y · Crystallinity · Differential thermal analysis · FCC

Introduction

A fluid catalytic cracking (FCC) catalyst is a porous microsphere containing zeolite Y dispersed in a clay matrix (kaolin and alumina). Zeolite Y is the rate-controlling constituent during the process of catalyst cracking and the matrix performs both physical and catalytic functions. Hence, its stability is crucial to the rigors of the cracking process. Heavy metals existing in petroleum feedstock, such as vanadium and nickel, have the most significant impact on the performance of FCC catalysts [1]. During the cracking process, these metals are deposited in the catalyst and affect both catalyst and selectivity. Vanadium species have mobility, mainly in the presence of steam, and can migrate onto the surface of zeolite to destroy its structure.

Extensive research on FCC has focused on understanding the destructive role of vanadium, since it is a major issue for catalyst performance during the cracking of residuum-containing feeds [2–4].

The FCC process plays an important role in heavy oil upgrading. It converts heavy petroleum fractions into valuable light products such as gasoline and diesel. Over the years, many improvements have been made in the FCC process. The development of a very active zeolite cracking catalyst allowed FCC reactions to be completed in short contact times in riser reactors [5]. Since the FCC is a catalytic and heat integration process, efforts have been devoted to establish the FCC feedstock specification to meet process constraints such as catalyst deactivation and heat load requirements. To meet these requirements, the metal and carbon residue (coke) contents of feedstock are kept at certain levels.

Thermogravimetry (TG) and differential thermal analysis (DTA) are the most employed techniques of thermal analysis [6]. In a DTA technique, the sample and the reference material are in little crucibles supported on thermocouples which measure the temperatures during the heating schedule. If the sample undergoes endothermic event, its temperature will lag behind the reference temperature, which follows the heating schedule. The output from the thermocouples recording the temperature will consist of a signal. If an exothermic process occurs in the

---

M. L. A. Gonçalves (✉) · M. D. Vieira
Chemistry Institute, Universidade Federal Fluminense, Outeiro de São João Batista, s/n, Centro, Niterói, RJ 24020-150, Brazil
e-mail: luisa.aleixo@infolink.com.br

D. A. P. Mota · W. V. Cerqueira · A. M. R. F. Teixeira
Pos Graduation Program in Chemistry, Universidade Federal Fluminense, Outeiro de São João Batista, s/n, Centro, Niterói, RJ 24020-150, Brazil

sample, the response will be a signal in the opposite direction. The DTA curves are registered in $\Delta T \times$ Temperature of sample. But as thermocouples are used to measure the temperature, sometimes the results are expressed by voltage variation (μV or μVg^{-1}). The area of the signal can be converted in energy unit ($J\ g^{-1}$) with metal standard calibration.

TG and DTA have been employed to evaluate catalysts, providing valuable information about stability and changes in heat [7–12]. However, DTA has not been successful in providing a general, reproducible, and standard method for measuring and recording thermal stability. Many factors affect the temperature at which the event is observed. Therefore, it is useful only for direct comparisons, i.e., to obtain data using the same device and under the same conditions.

This paper aims to show that TG/DTA simultaneous techniques are sensitive techniques that enable one to observe differences in the crystalline structure of zeolite catalysts. Our study compares the variation of the collapse energy of the crystalline structure in a fresh zeolite catalyst and that of the same structure in vanadium impregnated catalyst.

Experimental procedure

Samples

A sample of fresh FCC catalyst (CAT-F) containing zeolite Y dispersed in an inert matrix of kaolin and Al_2O_3 was selected for this study. Pure catalytic components (zeolite Y, kaolin and Al_2O_3) were also selected.

The basic characteristics of the CAT-F sample were provided by the manufacturer and are summarized in Table 1.

A sample containing vanadium and nickel catalyst (CAT-I) was prepared with CAT-F impregnated with vanadium and nickel, following the method described by Mitchell [13]. Prior to metal impregnation, the CAT-F was activated at 540 °C and, after impregnation with vanadium naphtenate and nickel naphtenate, it was calcined at 600 °C for 3 h, to eliminate organic material. The amount of vanadium and nickel—3000 μg of each metal per gram of catalyst—was chosen based on the traditional cyclic impregnation and aging treatment for activity studies. In the Mitchell methodology, after impregnation the catalyst is deactivated by steam. However, since the objective of our study was to observe differences in the catalyst only in response to the addition of metal, steam was not introduced here.

Table 1 Characteristics of fresh catalyst (CAT-F) under study

Properties	Values
Total area/m^2/g	337
Particle medium size (micra)	76
Apparent density/g/cm^3	0.72
Pore volume/cm^3/g	0.34
Na/p/p	0.31
Fe_2O_3/p/p	0.44
P_2O_5 (μg/mg)	0.70
Al_2O_3/p/p	40.7

A sample, which we will refer to as CAT-$F_{treated}$, was prepared by treating CAT-F at the same temperatures proposed by Mitchell, but without the addition of organometallic compounds. The objective was to observe the effect of temperature on the fresh catalyst.

Thermogravimetry and differential thermal analysis

All the experiments were conducted in a Netzsch STA-Luxx 409 thermal analyzer, using alumina crucibles (300 μL) at a heating rate of 50 K min^{-1} and an initial sample weight of 80 mg. Dynamic atmosphere of N_2 at 100 mL min^{-1} from 35 to 1200 °C was used. The sample's temperature was measured with a thermocouple attached directly to the crucible, i.e., very close to the sample. The temperature and the relation of peak area and energy were calibrated with nickel, gold and aluminum. So the calculation of the area of the exothermic event in DTA curves is expressed in energy units per gram of sample ($J\ g^{-1}$).

The STA-Luxx 409 simultaneous thermal analyzer allows for simultaneous thermogravimetric and differential thermal analysis (TG/DTA). Its use therefore enabled us to monitor the mass loss of the catalyst during heating. The release energy was calculated based on the mass at the beginning of the exothermic event. This calculation was made possible by the simultaneous TG/DTA analysis. To facilitate viewing, we used the resources of a data handling program which allows the DTA curve to be adjusted so that it starts at 0 mW/mg.

X-ray diffraction

The X-ray diffraction patterns were recorded on a BRUCKER D8 diffractometer using CuK_α radiation from 3 to 70° at step of 0.5° at 3 s/step.

The samples crystallinity was calculated based on ASTM 3906-03 methodology [14]. The XRD patterns of the sample and the reference are obtained under the same conditions. The fresh catalyst was considered as a reference sample (100% crystalline). The sample's X-ray diffraction intensities of the (533) peak (23.5°) are compared to provide %XRD intensity/reference CAT-F (533). The intensity ratio, expressed a percentage of crystallinity

$$\%\text{XRD crystallinity} = \frac{\text{Y-zeolite peak intensity in the sample}}{\text{Y-zeolite peak intensity in the CAT-F}} \times 100$$

Results and discussion

During the FCC process, the catalyst is subjected to high temperatures, and during the cracking process, metals are deposited in the catalyst, affecting both catalysis and selectivity. To study the influence of metals on the crystalline structure of the catalyst, a fresh catalyst (CAT-F) was impregnated vanadium and nickel using Mitchell's procedure, which simulates metal impregnation of catalysts in a FCC process. Therefore, to study the influence of temperature by the Mitchell procedure during metal impregnation, the CAT-F was heated in controlled furnace at 540 °C for 3 h to release water and at 600 °C for 6 h (CAT-$F_{treated}$). All the samples—CAT-F, CAT-$F_{treated}$, and CAT-I—were then analyzed by TG/DTA to observe their thermal behavior with respect to mass and energy variations resulting from the different events to which the samples were subjected.

The resulting TG/DTA curves indicated that CAT-F sample (Fig. 1a) underwent two different events. The first was caused by the evolution of bound water (120–400 °C) and the second by strongly bound water (400–550 °C) present in the components of the catalyst [15, 16]. The DTA curve of CAT-F (Fig. 1a) shows two endothermic signals and a very weak exothermic signal between 1000 and 1150 °C. The third signal is clearly visible in an enlarged graph (Fig. 1b). To facilitate visualization, we used a data handling feature that allows the DTA curve to be adjusted to start at 0 mW/mg. Under these conditions, the exothermic signal revealed the occurrence of two events.

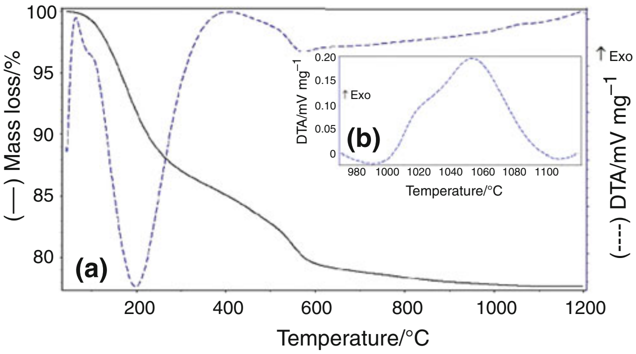

Fig. 1 TG/DTA curves of (*a*) CAT-F sample and (*b*) enlarged DTA curve at 980–1100 °C

An XRD analysis of the CAT-F sample indicated a pattern typical of crystalline substances (Fig. 2a), with sharp well-defined peaks with a signal characteristic of zeolite Y [17]. The diffractogram of the residual mass, i.e., after it was subjected to a temperature of 1200 °C, in TG/DTA, showed an amorphous substance (Fig. 2b), indicating the complete destruction of the crystalline structure of the catalyst, confirming that the exothermic signal in DTA curve represents the destruction of the zeolite Y's crystalline structure and corroborates with what is shown in the literature [18–22].

After the metal impregnation, the CAT-I sample was analyzed by TG/DTA. The resulting TG curves (Fig. 3a) revealed that a mass loss occurred between 120 and 400 °C, but no significant mass loss between 400 and 550 °C. The phenomenon was attributed to the fact that the catalyst was heated at 650 °C during the metal impregnation procedure, when it lost its bound and strongly bound water. As expected, the DTA curve showed only one endothermic signal and an exothermic signal of low intensity when compared with the same signal observed in the CAT-F curve. The profile of the exothermic signal, which is clearly visible in an enlarged graph (Fig. 3b), suggests two events, as in the CAT-F sample.

The DTA curve of the CAT-$F_{treated}$ sample (Fig. 4a) showed only one endothermic signal corresponding to the loss of humidity, and a very weak exothermic signal between 1000 and 1150 °C. Like the CAT-F and CAT-I samples, the exothermic signal is more clearly visible in the enlarged region between 950 and 1120 °C in the graph (Fig. 4b).

The released energy represented by the exothermic signal in the DTA curves was calculated by determining the peak area based on the mass at the beginning of the exothermic event of the CAT-F, CAT-I, and CAT-$F_{treated}$ samples. Three replicates of each sample were recorded for a reproducibility study. The average area of the exothermic peak in CAT-F was 12.8 J/g, while CAT-$F_{treated}$ and CAT-I showed 10.7 and 8.6 J/g, respectively. The average values were compared statistically leading to the conclusion that the three samples showed different values [23]. As can be seen, the areas in CAT-F show changes after heat treatment and metal impregnation. The phenomenon was observed in prior work when pure zeolite Y was impregnated with vanadium and nickel [24].

To identify the origin of the two signals present in the DTA exothermic signal, the three major catalyst components—zeolite Y, kaolin, and alumina—were analyzed by TG/DTA to determine which components contributed to the occurrence of the exothermic signals at 980 and 1200 °C.

Fig. 2 X-ray diffraction patterns of (*a*) CAT-F and (*b*) CAT-F after subjected to a Temperature of 1200 °C in TG/DTA

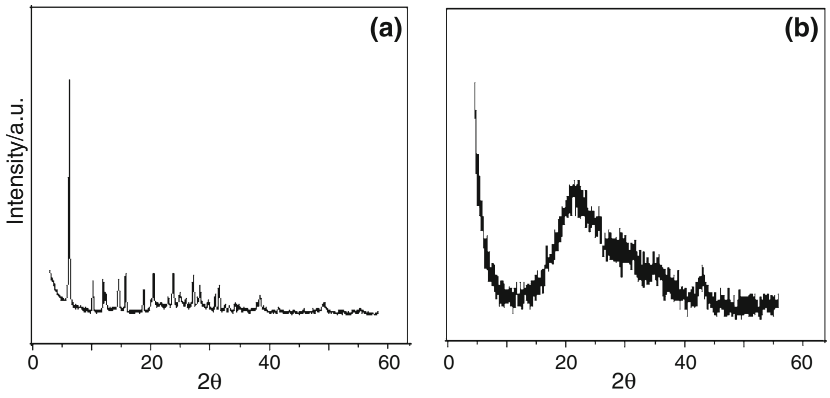

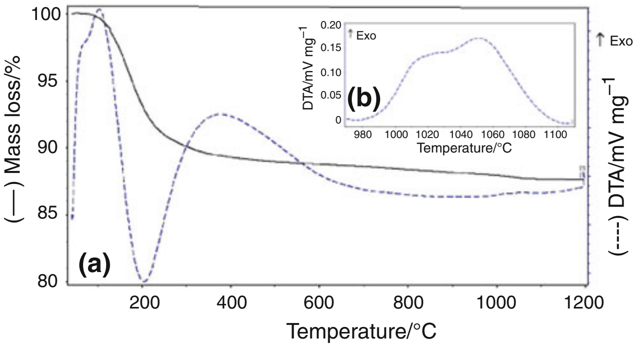

Fig. 3 TG/DTA curves of (*a*) CAT-I sample and (*b*) enlarged DTA curve at 980–1100 °C

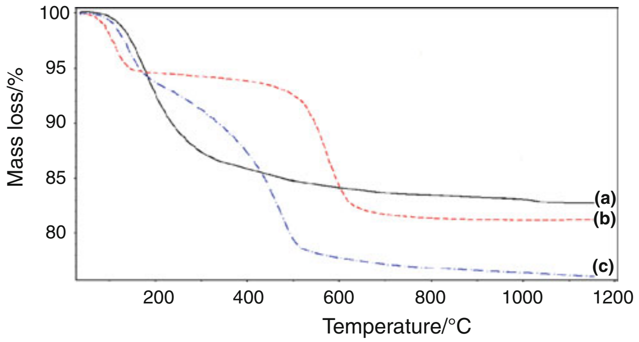

Fig. 5 TG curves of (*a*) Y zeolite, (*b*) kaolin, and (*c*) alumina at 50 K min^{-1} in N_2 flow (50 mL min^{-1})

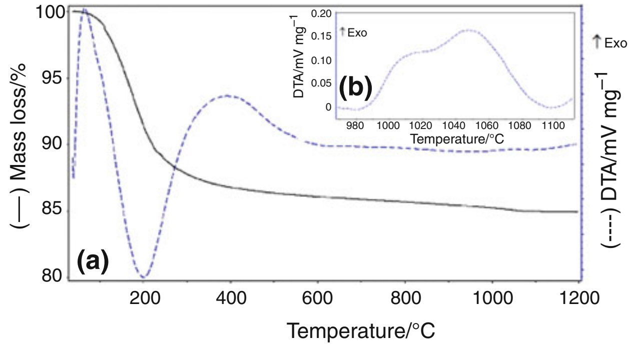

Fig. 4 TG/DTA curves of (*a*) CAT-$F_{treated}$ sample and (*b*) enlarged DTA curve at 980–1100 °C

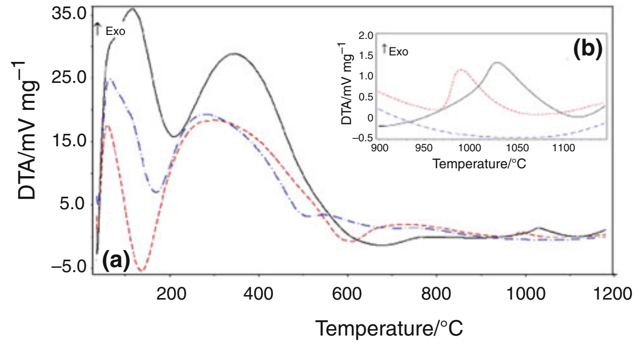

Fig. 6 (*a*) DTA curves of Y-zeolite, kaolin, and Al_2O_3 samples at 50 K min^{-1} in N_2 flow (50 mL min^{-1}); (*b*) Enlarged DTA curves at 900–1150 °C

The TG curves in Fig. 5 indicate that Y kaolin and alumina lost bound water (120–400 °C) and strongly bound water (400–550 °C), while the zeolite sample lost only adsorbed water. The DTA curves of the three components show endothermic events involved in energy-related water release, as mentioned previously (Fig. 6a). However, the kaolin and zeolite Y presented an exothermic event at 950–1150 °C, which is clearly visible in the magnified curve in the region of 950–1200 °C (Fig. 6b). These events represented a rapid reorganization of oxide ions in the kaolin lattice structure [15] and the collapse of the zeolite Y structure [19, 20]. The highest exothermic event in kaolin occurred at 980 °C and in zeolite Y at 1130 °C. The peak area of zeolite collapse represents 152 J/g and the kaolin lattice reorganization, 41 J/g. The energy release to zeolite collapse is fourfold higher than that of the kaolin reorganization.

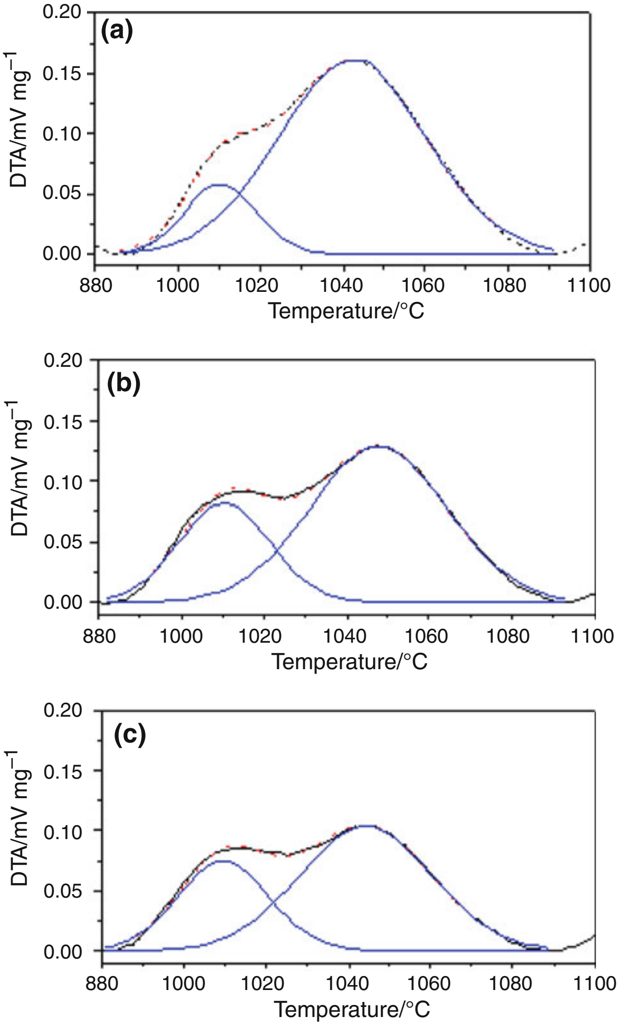

Fig. 7 Deconvolution of DTA peaks (*a*) CAT-F (*b*) CAT-F$_{treated}$ and (*c*) CAT-I

Table 2 Peak area of peak 1 and peak 2 after deconvolution calculation

SAMPLE	Peak 1 area/J/g	Peak 2 area/J/g	Total area/J/g
CAT-F	2.0	10.9	12.8
CAT-F$_{treated}$	3.2	7.5	10.7
CAT-I	2.9	5.7	8.6

Therefore, in the DTA conditions employed here to analyzed catalyst samples, the first signal observed in catalyst samples at an initial temperature of about 1000 °C was attributed to a reorganization of the kaolin structure, and the second, which overlapped the first at approximately 1028 °C, was attributed to the collapse of the zeolite Y crystalline structure.

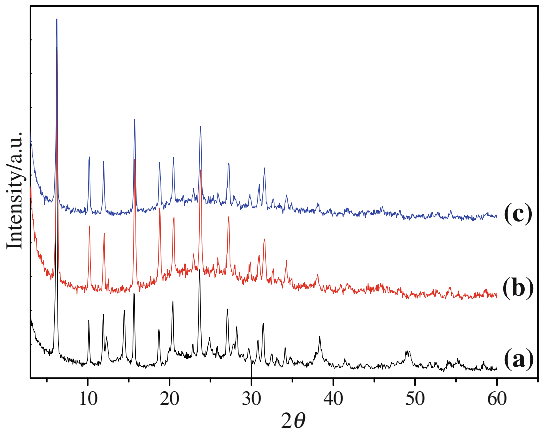

Fig. 8 X-ray diffraction patterns of (*a*) CAT-F (*b*) CAT-F$_{treated}$ and (*c*) CAT-I

Table 3 Comparison of crystallinity os CAT-F, CAT-F$_{treated}$, and CAT-I obtained by DTA and XRD

Sample	Crystallinity (%)	
	DTA	XRD
CAT-F	100	100
CAT-F$_{treated}$	69	75
CAT-I	52	64

The overlapping peaks in the CAT-F, CAT-I, and CAT-F$_{treated}$ DTA curves were separated using a Gaussian peak profile (Fig. 7), which indicated that the highest contribution of energy came from zeolite Y. Thus, after deconvolution, the area of the second exothermic signal indicated the amount of energy released during the collapse of the zeolite Y structure, and its intensity was assumed to be proportional to the integrity of the three-dimensional structure in the catalyst.

The area of the second exothermic signal of a fresh catalyst (CAT-F) was taken as a reference, and any alteration of this value was considered a modification in the zeolite Y crystalline structure. All the DTA curves presented here were treated equally to allow for their comparison.

Table 2 showed the results after calculation. Thus, 10.9 J/g corresponded to 100% of crystalline zeolite Y present in the CAT-F. On the other hand, the value found for the CAT-F$_{treated}$ sample indicated that the zeolite Y in CAT-F lost 31% of its crystallinity after thermal treatment, while the CAT-I sample indicated a loss of 48% of its crystallinity. The temperature employed during metal impregnation appeared to affect the crystalline structure of zeolite Y in the catalyst, as did the introduction of metal. These observations, which are based on the DTA curve, lead us to believe that heat treating the catalyst at the temperatures of metal impregnation causes a partial loss of the crystallinity of zeolite Y and that this loss of crystalline structure increases after the addition of metals.

To confirm the hypothesis that the three catalyst samples still retained a certain state of crystallinity after heat treatment and metal impregnation, the samples were analyzed by XRD. The resulting diffractograms (Fig. 8) revealed patterns of typical crystalline structures with sharp well-defined peaks, indicating that all three samples still retained a certain state of crystallinity after temperature and impregnation with metal. The samples crystallinity was calculated based on ASTM 3906-03 methodology [14] and assuming that the fresh catalyst (CAT-F) was 100% crystalline, the crystallinity of the other samples was affected in response to the treatments, decreasing after the heat treatment and metal impregnation (Table 3). These differences may have resulted from the introduction of the metal. Be that as it may, the DTA technique displayed good sensitivity for detecting minor differences in the area of measurement of the collapse of crystalline structures.

A comparison of the XRD and DTA results (Table 3) indicates that the sensitivity of the DTA technique sufficed to reveal the crystalline modifications in the catalyst caused by temperature and metal impregnation. It is known that vanadium species are mobile, particularly in the presence of steam, and can migrate onto the surface of zeolite to destroy its structure [3]. Steam was not used in this study, although it is the main factor responsible for destroying the crystalline structure of zeolite Y. However, even without the presence of steam, DTA, like XRD, revealed changes in the zeolite Y structure after the introduction of metal. Cristiano-Torres et al. [25] presented recent results showing that vanadium can migrate on zeolite surface without water required for that movement and proved in their experiments that vanadium drastically affect catalyst selectivity.

Conclusions

The DTA technique proved sufficiently sensitive to detect slight changes in the integrity of three-dimensional structures in catalysts. Although this technique did not provide reproducible results for thermal stability measurements, it proved satisfactory for straightforward comparisons. The results presented here confirm the relevance of conducting more in-depth studies to correlate the collapse energy of zeolite Y in a specific catalyst with its resistance to high vanadium concentrations. Our studies to correlate the area of the exothermic signal obtained by the DTA curve and catalyst stability results obtained by traditional methods are ongoing.

Acknowledgements The authors thank CNPq/PROSET (Conselho Nacional de Desenvolvimento Científico e Tecnológico/Programa Setorial de Petróleo) and PETROBRAS (Brazilian Oil Company).

References

1. Wormsbecher RF, Peters AW, Maselli JM. Vanadium poisoning of cracking catalysts: mechanism of poisoning and design of vanadium tolerant catalyst system. J Catal. 1986;100:130–7.
2. Trujillo CA, Uribe UN, Knops-Gerrits PP, Oviedo LA, Jacobs PA. The mechanism of zeolite Y destruction by steam in the presence of vanadium. J Catal. 1997;168:1–15.
3. Xu M, Liu XX, Madon RJ. Pathways for Zeolite Y destruction: the role of sodium and vanadium. J Catal. 2002;207:237–46.
4. Liu C, Deng Y, Pan Y, Zheng S, Gao X. Interactions between heavy metals and clay matrix in fluid catalytic cracking catalysts. Appl Catal A. 2004;257:145–50.
5. Harding RH, Peters AW, Nee JRD. New developments in FCC catalyst technology. Appl Catal A. 2001;221:389–96.
6. Wendlandt WW. Thermal analysis. 3rd ed. New York: Wiley; 1986.
7. Liu J, Zhao Z, Xua C, Duana A, Zhub L, Wang X. Diesel soot oxidation over supported vanadium oxide and K-promoted vanadium oxide catalysts. Appl Catal B. 2005;61:36–46.
8. El-Toufailia FA, Wiegnerb JP, Feix G, Reichert KH. Optimization of simultaneous thermal analysis for fast screening of polycondensation catalysts. Thermochim Acta. 2005;432:99–105.
9. Crivello M, Péreza C, Fernándeza J, Eimera G, Herreroa E, Casuscellia S, et al. Synthesis and characterization of Cr/Cu/Mg mixed oxides obtained from hydrotalcite-type compounds and their application in the dehydrogenation of isoamylic alcohol. Appl Catal A. 2007;317(1):11–9.
10. Habersberger K. Thermoanalytical investigation of zeolites and related compounds. Thermochim Acta. 1987;110:337–41.
11. Pérez YO, Forero LAP, Cristiano-Torres DV, Trujillo CA. Brønsted acid site number evaluation using isopropylamine decomposition on Y-zeolite contaminated with vanadium in a simultaneous DSC–TGA analyzer. Thermochim Acta. 2008;470:36–9.
12. Fan W, Wei S, Yokoi T, Inagaki S, Li J, Wang J, et al. Synthesis, characterization and catalytic properties of H-Al-YNU-1 and H-Al-MWW with different Si/Al ratios. J Catal. 2009;266:268–72.
13. Mitchell BR. Metal contamination of cracking catalysts. 1. Synthetic metals. Ind Eng Chem Prod Res Dev. 1980;79:209–13.
14. American Society for Testing, Materials (ASTM-3906–03). Standard test method for determination of relative X-ray diffraction intensities of Faujasite-type zeolite-containing materials. West Conshohocken: ASTM; 2003.
15. Mayoral MC, Isquierdo MT, Andrés JM, Rubio B. Aluminosilicates transformations in combustion followed by DSC. Thermochim Acta. 2001;373:173–80.
16. Yang X, Sun Z, Wang D, Forsling W. Surface acid–base properties and hydration/dehydration mechanisms of aluminum (hydr)oxides. J Colloid Interface Sci. 2007;308:395–404.
17. Xu B, Rotunno F, Bordiga S, Prins R, Van Bokhoven JA. Reversibility of structural collapse in zeolite Y: alkane cracking and characterization. J Catal. 2006;241:66–73.
18. Trigueiroa FE, Monteiro DFJ, Zotin FMZ, Sousa-Aguiar EF. Thermal stability of Y Zeolites containing different rare earth cations. J Alloys Compd. 2002;344:337–41.
19. Zi G, Yi T, Yugin Z. Effect of dealumination defects on the properties of Y zeolite. Appl Catal. 1989;56:83–94.
20. Kosanovic C, Subotic B, Smit I. Thermally induced phase transformations in cation-exchanged zeolites 4A, 13X and synthetic mordenite and their amorphous derivatives obtained by mechanochemical treatment. Thermochim Acta. 1998;317:25–37.
21. Giuseppe C. Zeolites upon heating: factors governing their thermal stability and structural changes. J Phys Chem Solids. 2006;67:1973–94.

22. McDaniel CV, Maher PK. Zeolite stability and ultrastable zeolites. In: Rabo JA, editor. Zeolite chemistry and catalysis. 2nd ed. ACS Monograph 171. American Chemical Society: Washington, DC; 1979. p. 288.
23. Freund JE, Gary SA. Modern elementary statistics. Englewood Cliffs: Prentice-Hall, Inc.; 1997.
24. Gonçalves MLA, Vieira MD, Cerqueira WV, Teixeira AMRF. A tool for predicting the integrity of Y zeolite crystalline structure by differential thermal analysis. J Therm Anal Calorim. 2009;97: 503–6.
25. Cristiano-Torres DV, Ozório-Pérez Y, Palomeque-Forero LA, Sandoval-Díaz LE, Trujillo CA. The action of vanadium over Y zeolite in oxidant and dry atmosphere. Appl Catal A. 2008;346: 104–11.